ELSEVIER

Ceramics International 28 (2002) 541–547

CERAMICS INTERNATIONAL

www.elsevier.com/locate/ceramint

# Preparation of MCM-41 with high thermal stability and complementary textural porosity

Huxing Chen*, Yingchun Wang

*College of Materials Science and Chemical Engineering, Zhejiang University, Hangzhou 310027, PR China*

Received 22 May 2001; received in revised form 13 August 2001; accepted 11 December 2001

**Abstract**

Preparation of mesoporous molecular sieve MCM-41 with complementary textural porosity and high thermal stability that results from thicker wall has been achieved by decreasing surfactant/silicon ratio of synthesis gel. MCM-41 material obtained by using the surfactant/silicon molar ratio of 0.10 consists of large and well-defined spherical particles. A further decrease in the ratio results in the formation of MCM-41 silica with the bimodal framework meopores and complementary textural porosity. The textural porosity results from the loose aggregate structure. The resultant materials retain ordered channels and large BET surface area even after thermal treatment at 1273 K for 1 h in air. The complementary textural porosity decreases the length of the one-dimensional mesopores and provides the facilitating framework access for the diffusion of mass. © 2002 Published by Elsevier Science Ltd and Techna S.r.l.

*Keywords:* MCM-41; Thermal stability; Complementary textural porosity; Thicker wall; Surfactant/TEOS

## 1. Introduction

The ordered mesoporous molecular sieve MCM-41 with the special characteristics of large internal surface area and favorable uniformity but ease controllable size of the pore [1] has attracted considerable interest in physics, chemistry, materials science, and other relevant areas [2,3]. This novel mesoporous solid is desirable as shape/size selective adsorbents [4], hosts for quantum structures [5], catalysts [6], and catalyst supports [2]. However, the range of application has been limited by the instability of the pore structure of the mesoporous materials. Some authors reported that the structural instability of MCM-41 is due to the hydrolysis of the bare Si–O–Si(Al) bonds in the presence of adsorbed water [7–9]. For example, the ordered mesoporous structure was completely lost on exposure to the air even at room temperature for three months resulting from silicate hydrolysis [9], although both pure-silica and aluminosilicate MCM-41 can be stable at as high as 1123 K in dry air or 1073 K in air with low water vapor pressure [10,11]. The structure of MCM-41 can also be destroyed under mechanical compression due to the mechanochemical hydrolysis of Si–O–Si bonds [7,8].

The stability of mesoporous materials, fortunately, can be improved remarkably by increasing the hydrophobicity[7] or by increasing condensation of the silanol groups during the formation of the mesostructure [12]. The increase in the wall thickness also effectively results in stabilizing the ordered mesoporous structure against thermal and hydrothermal treatment [13,14]. To the best of our knowledge, the largest reported value of the pore wall thickness for MCM-41 directly synthesized is about 1.8 nm [15], although Al-containing MCM-41 with the wall thickness of 2.4 nm can be prepared by a post-synthesis alumination method [16].

The previously reported siliceous MCM-41 materials were synthesized from gels with surfactant/silicon molar ratios of more than 0.12 [17,18]. However, the lower ratio synthesis systems are of great interest for several reasons: decreasing the amount of expensive template used, increasing the thickness of framework wall, and improving in the structural stability from the increased wall thickness. Here we report a direct and highly efficient synthesis route to the high thermal stability MCM-41 which structural ordering can be retained even after thermal treatment at 1273 K in air.

* Corresponding author.

0272-8842/02/$22.00 © 2002 Published by Elsevier Science Ltd and Techna S.r.l.
PII: S0272-8842(02)00007-X

## 2. Experimental

### 2.1. Syntheses of materials

The source of silicon was tetraethyl orthosilicate (TEOS, 98%). The structure-directing agent was cetyltrimethylammonium bromide (CTAB). A typical synthesis gel was prepared by adding 5.78 g of TEOS to an aqueous solution containing 1.01 g of CTAB and 0.34 g of NaOH and 30 ml of deionized water. After further stirring for about 1 h at room temperature, the resulting homogeneous mixture was crystallized under static hydrothermal conditions at 383 K in a Teflon lined autoclave for 96 h. The molar composition of the initial gel mixture was 1.0:0.10:0.30:60 TEOS/CTAB/NaOH/$H_2O$. The solid product was obtained by filtration, washed with deionized water, dried in air at 353 K and calcined in air at 813 K for 24 h to remove the CTAB. The effect of surfactant/silicon ratios and hydrothermal crystallization times on mesoporous structure was also described. The compositions used to synthesize examples are shown in Table 1.

### 2.2. Characterization

The thermal stability of the above samples was investigated by following intensity changes in X-ray diffractograms as a function of the calcination temperatures in air. The hydrothermal stability was investigated by mixing ca. 0.5 g of the calcined sample with 50 g distilled water and heating at 373 K for 50 h under reflux conditions. After hydrothermal treatment, the samples were filtered, washed with deionized water and dried at 363 K overnight. The hydrothermal stability was determined with the peak intensities of the XRD patterns.

The XRD patterns were obtained with a Cu$K_\alpha$ radiation (40 kV, 60 mA) using a Rigaku D/MAX-αB instrument at 0.002° step size and 0.24 s step time over a $1.8° < 2\theta < 10°$ range. The samples were prepared as thin layers on metal slides.

$N_2$ adsorption isotherms were measured at 77 K on a Micromeritics ASAP 2400 analyzer using standard continuous procedures, and samples were first degassed at 573 K for 5 h. Surface areas were determined by BET method in the 0.05–0.31 relative pressure range [19,20], and the pore size distribution was determined by the Barrett–Joyner–Halenda (BJH) formula [21–23]. The mesopore parameters were obtained from the pore size distribution curves.

Scanning electron micrographs were obtained from an ETMA 8705QH Electron Bean Probe. Samples were deposited on a sample holder with an adhesive carbon foil and sputtered with gold.

Table 1
Composition of synthetic mixtures

| Sample | Molar composition TEOS/CTAB/NaOH/$H_2O$ |
|---|---|
| MCM-41(10) | 1.0:0.10:0.30:60 |
| MCM-41(08) | 1.0:0.08:0.30:60 |
| MCM-41(06) | 1.0:0.06:0.30:60 |

## 3. Results and discussion

### 3.1. XRD

Fig. 1 shows the powder XRD patterns of samples obtained at 383 K for 96 h from different gels. The XRD pattern of the as-synthesized MCM-41(10) exhibits a high-intensity peak and four additional higher order peaks having *d* spacings consistent with hexagonal indexing (Fig. 1, curve a). This suggests that hexagonal mesoporous material with a high degree of long range ordering of the structure and well-formed hexagonal pore arrays can be prepared in low surfactant/silicon molar ratio synthesis system. Upon calcination at 813 K for 24 h, the intensity of the XRD peaks increases by about 2.3 times, the full width of the (100) peak at the half maxima reduces, and the resolution of the higher order peaks is improved (Fig. 1, curve b), as compared to the as-synthesized sample. These results reflect that the degree of ordering is dramatically improved by the removal of the surfactant. Moreover, the lattice distance contraction of as low as 2.8% is considerably less than the value (about 5%) obtained for any previously reported MCM-41 materials synthesized in high ratio synthesis systems [11], indicating that mesoporous material obtained in the synthetic system with the lower molar ratio of the surfactant to silicon is thermally more stable. For the calcined MCM-41(10) after thermal treatment at 1273 K for 1 h, as seen from the XRD pattern f (Fig. 1B), one intense peak with ad spacing of 3.30 nm is still clearly observed, suggesting the presence of ordered structure of the pore even at 1273 K. On the contrary, MCM-41 materials produced with the high surfactant/silicon ratios show no X-ray peaks at the high temperature of 1273 K [11]. This further confirms the high thermal stability of the mesoporous structure. However, the structure of MCM-41 was completely lost upon boiling in water for 50h (Fig. 1, curve e).

An increase of TEOS content in the initial gel from 5.78 to 7.52 g results in a material (surfactant/silicon, 0.08) which is no longer mesoporous due to the production of the excess ethanol from the hydrolysis and condensation of TEOS. In contrast, the material prepared with the reduced amounts of surfactant in the initial gels still remains ordered mesoporous even when the surfactant/silicon ratio is changed from 0.08 to 0.06

(Fig. 1A, curves c and d, respectively). It can be seen from the curves that with the ratio decreas the calcined products exhibit a gradual reduction in the intensity of XRD pattern and lack the higher order (210) and (310) peaks. From Fig. 1B, we can see that both the $d_{100}$ spacing and the intensity of the (100) peak of MCM-41(08) after treated at 1273 K for 1 h are higher than that of the treated MCM-41(10), which suggests that MCM-41(08) is thermally more stable than MCM-41(10). Although the $d_{100}$ spacing of MCM-41(06) after treated at 1273 K for 1 h is higher than that of the treated MCM-41(10), the intensity of (100) peak of the former is much lower than that of the later, indicating that the further decrease in the ratio less than 0.08 does not increase the thermal stability.

The mesophases originating from the same initial gels of 1.0:0.10:0.30:60 TEOS/CTAB/NaOH/$H_2O$ were sampled at different reaction times between 0 and 144 h under typical hydrothermal conditions and give the XRD patterns shown in Fig. 2. As-synthesized and calcined samples are shown in Fig. 2A and B, respectively. After all reactants were mixed together at room temperature only for 1 h, an initial precipitate was formed and shows a tubular mesostructure with a $d_{100}$ spacing of 4.18 nm (Fig. 2, curve a). Upon calcination, these tubular mesophases show only a broad XRD peak corresponding to 3.86 nm (Fig. 2, curve e), indicating that these mesophases are not very stable. After hydrothermal reaction at 383 K, the tubular mesophase converts into a hexagonal MCM-41 mesophase. Moreover, with increasing hydrothermal reaction time, the intensity of the (100) peak increases, the full width at half maxima reduces, and the higher order peaks are observed. These results are in agreement with the liquid crystal (LC) templating mechanism [1]. When the concentration of surfactant used is far below the critical micelle concentration (CMC) required for hexagonal LC formation, the cylindrical surfactant and the silica aggregates are simultaneously formed, and further silicate condensation mediates the ordering of the cylindrical surfactant into the hexagonal arrangement.

### 3.2. $N_2$ adsorption isotherms and SEM

The $N_2$ adsorption–desorption isotherms and the BJH pore size distribution curves for calcined MCM-41 silicas, which were prepared from the low surfactant/silicon ratio synthesis systems, are shown in Fig. 3. The information derived from the isotherms is in agreement with the XRD patterns (Fig. 1). The curve for the calcined MCM-41(10) material is a typical reversible type IV adsorption–desorption isotherm (Fig. 3a). The adsorption at low relative pressure ($p/p_0 < 0.3$) is from the monolayer adsorption of nitrogen on the wall of the

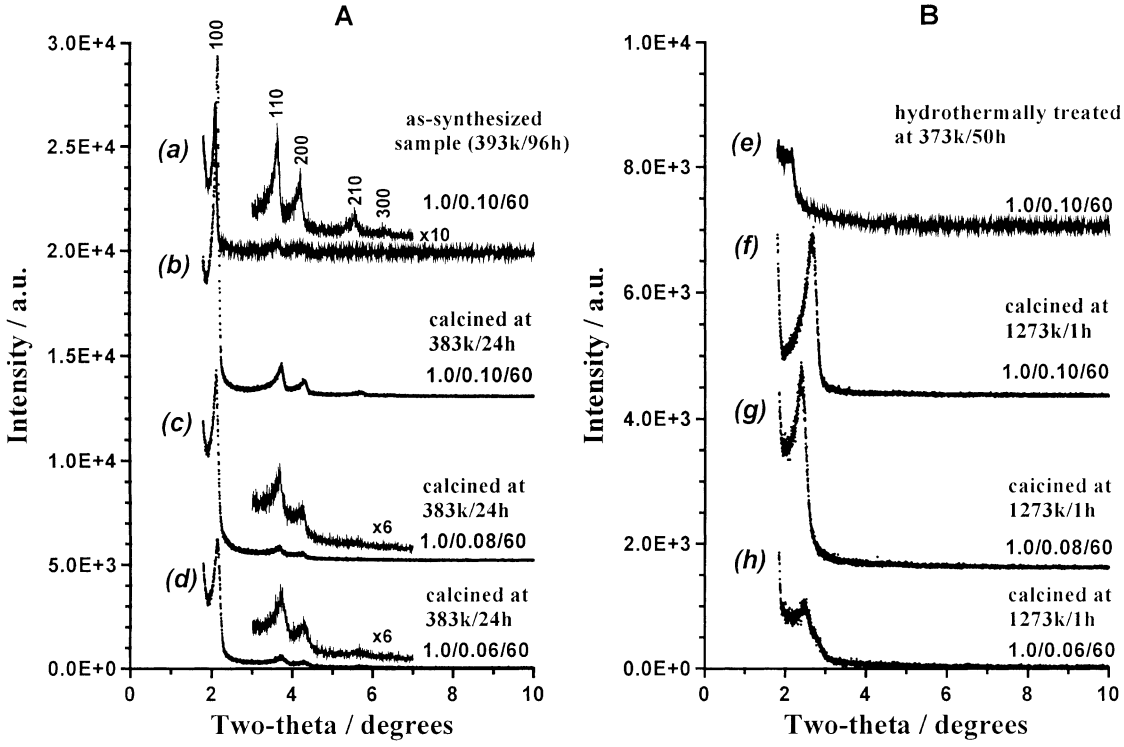


Fig. 1. A: powder XRD patterns of mesophases obtained at 383 K for 96 h from initial gels with different TEOS/surfactant molar ratios. (a) Is for as-synthesized sample, and (b), (c) and (d) are for samples calcined at 813 K for 24 h. B: powder XRD patterns of calcined samples after hydrothermal or thermal treatment. (e) Is for sample boiled in water for 50 h, and (f), (g) and (h) are for calcined samples heated at 1273 K for 1 h. The initial gel compositions are shown in the figure.

mesopores and does not imply the presence of any micropores. As the relative pressure increases ($p/p_0$), the isotherms exhibit sharp inflection, which is characteristic of capillary condensation within uniform mesopores, where the $p/p_0$ position of the inflection point is related to the diameter of the mesopore. Furthermore, the sharpness of the isotherm in range $0.3 < p/p_0 < 0.4$ corresponds to uniformity of mesopore size. The hysteresis loop in nitrogen adsorption–desorption isotherm at low relative pressure ($\sim$0.3) reflects the characteristic of pore structure. Since MCM-41 has only one-dimensional uniform mesopores, it is clear that the hysteresis loop reflects its uniform mesopore diameter, which limits the emptying and filling of the accessible volume [15]. The BJH pore size distribution curve shows MCM-41(10) material with a quite narrow pore diameter distribution centered around 2.6 nm (Fig. 3a, inset). Thus, the framework walls are $\sim$2.0 nm thick (Table 2). Accordingly, the thicker framework walls result in Brunaer–Emmett–Teller (BET) surface area (871 $m^2/g$, Table 2) that is relatively lower than the values typically found for MCM-41 prepared in the high surfactant/silicon molar ratio systems (more than 1000 $m^2/g$). Coustel et al. [13] prepared MCM-41 samples with a maximum wall thickness of $\sim$1.8 nm. This is the reason that our calcined MCM-41(10) sample was thermally more stable than their most stable material. The BET surface area is still as much as 376 $m^2/g$ in the treated MCM-41(10) sample even after heating at 1273 K. In contrast, we find that the BET surface area for the previously reported siliceous MCM-41 material decreases to 14 $m^2/g$ when subjected to the same thermal treatment [11]. The type I of $N_2$ adsorption-desorption isotherm of the treated MCM-41(10) (Fig. 3b) clearly shows no mesopores but the presence of micropores with a total pore volume of 0.21 $cm^3/g$. Thus, the thermal treatment at 1273 K suffers a decrease in the pore diameter of MCM-41(10) from mesoporous to microporous dimensions. Although both the long ordering of mesoporous structure and the homogeneity of pore are improved at long hydrothermal reaction times, the positions of both XRD patterns (Fig. 2B) and maxima in the BJH plot (not shown) change very little with time. These results suggest that the framework wall thickness almost remains largely unaffected by the hydrothermal reaction time.

A similar trend is obtained for MCM-41(08) and MCM-41(06) samples prepared in the lower surfactant/silicon ratio systems (Fig. 3c and d, respectively). An important distinction between these two MCM-41 silicas and MCM-41(10) is the presence of the hysteresis loops at higher relative pressures ($>0.45$) which are a consequence of $N_2$ filling the textural mesopores [24,25]. In addition, for MCM-41(06) samples, the hysteresis loop at $p/p_0 > 0.9$ indicates that the macropores, which are associated with the presence of amorphous silica, are filled at high relative pressures (Fig. 3d). Surface areas determined by the BET method are close to 550 $m^2/g$ for

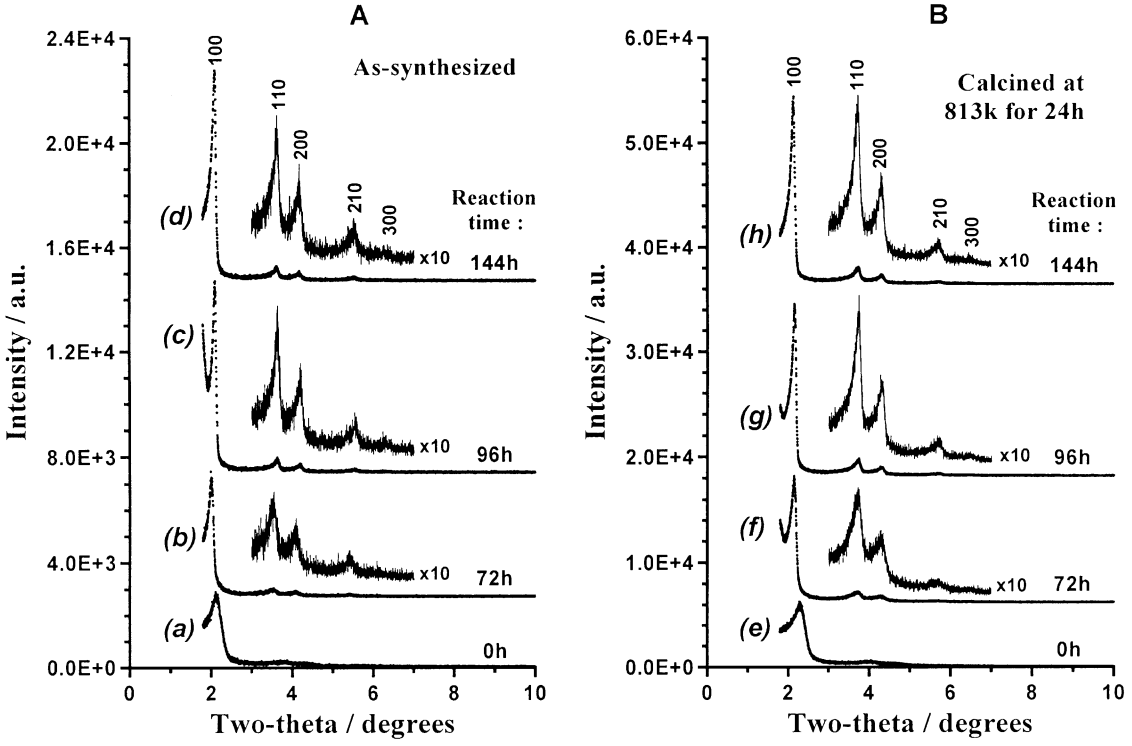


Fig. 2. Powder XRD patterns of mesophases obtained at 383 K for different reaction times from the same initial gel as 1.0:0.10:0.30:60 TEOS/CTAB/$NaOH/H_2O$. A: as-synthesized samples, B: calcined samples.

the both compounds, and the BJH pore size distribution curves verify the bimodal framework and textural pore size distributions, suggesting that these two compounds obtained with the lower surfactant/silicon ratio provide complementary textural porosity. Pore volumes are close to 0.65 $cm^3/g$ for both compounds. However, pore size distribution curves increase from 2.52 to 2.64 nm as the surfactant/silicon ratio is decreased from 0.08 to 0.06. Thus, the framework wall thickness of 2.27 nm for the MCM-41(08) is the largest among the three compounds (Table 2), which is in agreement with XRD results that the intensity and d spacing of MCM-41(08) are the largest upon thermal treatment at 1273 K (Fig. 1 and Table 2). These results indicated that the thick wall is resposible for the improved thermal stability of the mesoporous materials obtained in the synthestic systems with the low molar ratio of surfactant to TEOS.

SEM images showing the particle texture of MCM-41 silicas obtained from initial gels with various amounts of surfactant are displayed in Fig. 4. The surfactant/TEOS ratio of 0.10 provides MCM-41 silica with well-defined elementary spherical particles with mean size of about 8 μm and a few slit particles (Fig. 4a). The formation of large crystals of MCM-41 would be difficult due to the one-dimensional channel structure which is subject to bending and fracture [14]. The crystal size of normal MCM-41 specimens presented in previous reports [27] is in the range of 0.4–0.6 μm and no crystallites larger than 1 μm were observed. The crystal size of MCM-41 obtained by using calcined small crystallite MCM-41 as seeds in a multistage synthesis method [14] is from 4 to 8 μm. The result in this work suggests that preparation of large crystal MCM-41 can be directly achieved by using low molar ratio of surfactant/TEOS. However, the other materials synthesized with the lower surfactant/ TOES ratios, such as 0.08 (Fig. 4b) and 0.06 (Fig. 4c), exhibit structures with loose aggregates built of smaller and irregular-shaped elementary particles.

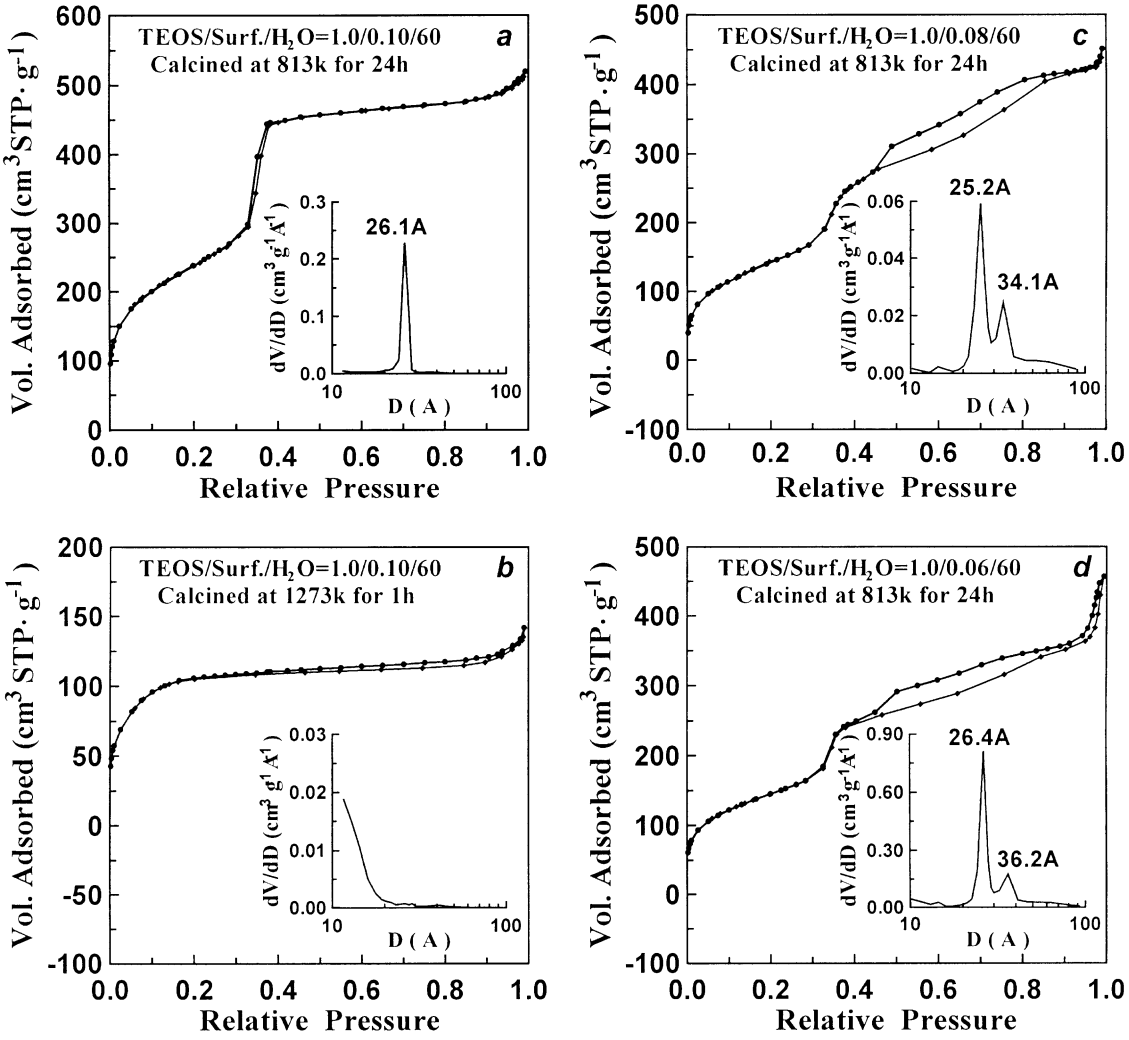


Fig. 3. Adsorption–desorption isotherms of nitrogen at 77 K on samples obtained in different TEOS/surfactant molar ratio reaction systems. The calcination temperature is 813 K for (a), (c), and (d). The thermally post-treatment temperature is 1273 K for (b). The inserts show the BJH pore size distribution calcined from the desorption branch of the isotherms.

Table 2
Physical properties of products calcined at 813 K

| Sample | $d_{100}$ (nm) | A(BET) ($m^2/g$) | V(BJH) ($cm^3/g$) | D(BJH)[a] (nm) | $a_0$[b] (nm) | Wall thickness[c] (nm) | $d$[d] (nm) |
|---|---|---|---|---|---|---|---|
| MCM-41(10) | 4.10 | 871 | 0.79 | 2.61 | 4.73 | 2.12 | 3.30 |
| MCM-41(08) | 4.15 | 560 | 0.67 | 2.52 | 4.79 | 2.27 | 3.70 |
| MCM-41(06) | 4.13 | 529 | 0.62 | 2.64 | 4.77 | 2.13 | 3.53 |

[a] D(BJH) = the maxima in the BJH pore size distribution.
[b] $a_0$ = The lattice parameter, from the XRD data using the formula $a_0 = 2d_{100}/\sqrt{3}$.
[c] Wall thickness = $a_0$-D(BJH).
[d] $d$ = Peak indices of calcined sample thermally heated at 1273 K for 1 h.

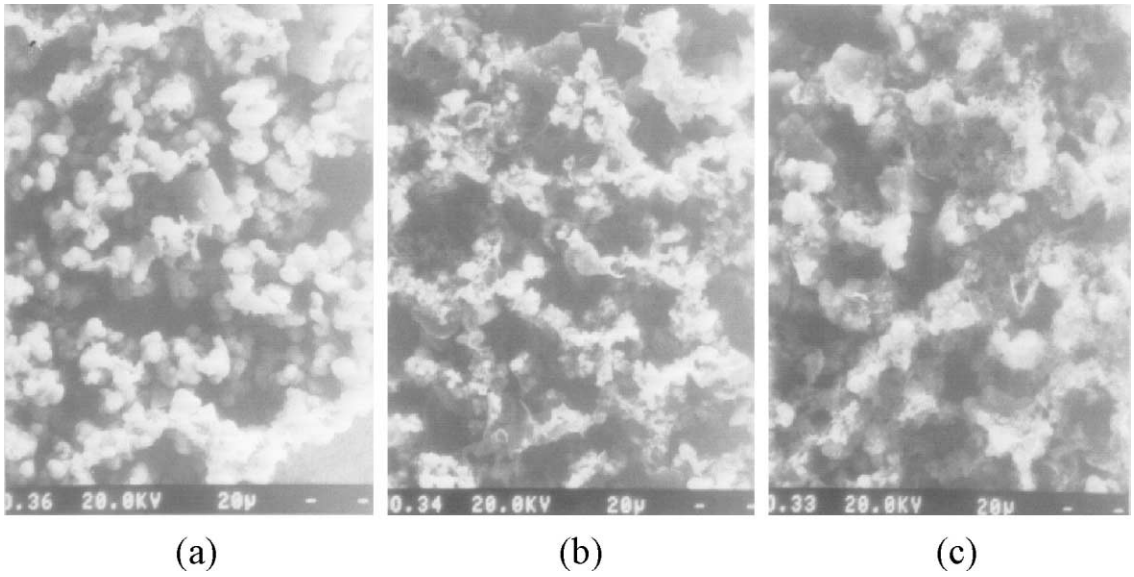


Fig. 4. SEM images of calcined samples obtained at 383 K for 96 h from initial gels with various amounts of surfactant. The surfactant/silicon ratios are (a) 0.10, (b) 0.08 and (c) 0.06. The scale bar is equal to the spacing between the white bars.

These materials are more suitable for catalyst supports, because the loose aggregate structures are believed to provide a significant complementary textural porosity as showen in Fig. 3, which decreases the length of the one-dimensional uniform mesopores and could be useful for improving the diffusion of mass in mesopores [26]. The mesostructures of large-particle restrict access to framework mesopores due to the long one-dimensional mesopores.

Stucky and co-workers [28] proposed that charge density matching at the surfactant inorganic interface controls the assembly process. They divided the global process into three reaction steps: multidentate binding of the silicate oligometers to the cationic surfactant, preferential silicate polymerization in the interface region, and charge density matching between the surfactant and the silicate. Following this mechanism, at the same concentration of silicate species, reducing the concentration of the surfactant correspondingly increases the number of the silicate species, which mediates the randomly ordered rodlike organic micelles to assemble the hexagonal mesophase. Therefore, MCM-41 with thicker wall and large particle can be obtained in the initial gels with the lower molar ratios of surfactant to silicon [such as MCM-41(10)]. However, a further decrease in the surfactant/silicon ratio causes the excess silicates aggregate anions which perturb the ordered mediating of the cylindrical surfactant and results in the formation of the mesoporous materials with complementary textural porosity [such as MCM-41(08) and MCM-41(06)] and even results in the formation of a small amount of amorphous silicas [such as the sample of MCM-41(06)].

## 4. Conclusions

It is shown in this work that the thermal stability of MCM-41 can be improved remarkably by using low molar ratio of surfactant/TEOS during the hydrothermal crystallization process. Calcined MCM-41 material obtained by using the ratio of 0.10 consists of large and well-defined spherical particles, which can retain the ordered channels and large BET surface areas

even after thermal treatment at 1273 K for 1 h in air. A further decrease in the ratio of surfactant/TEOS results in the formation of the mesoporous materials with the complementary textural porosity, which decreases the length of the one-dimensional mesopores and provides the facilitating framework access for the diffusion of mass. The thicker wall is believed to be responsible for the improved thermal stability of MCM-41. The complementary textural porosity results from the loose aggregate built of smaller and ill-defined elementary particles.

## References


[1] C.T. Kresge, M.E. Leonowicz, W.J. Roth, J.C. Vartuli, J.S. Beck, Nature 359 (1992) 710–712.
[2] K. Moller, T. Bein, Chem. Mater. 10 (1998) 2950–2963.
[3] J.K. Ying, C.P. Mehnert, M.S. Wong, Angew. Chem. Int. Ed. 38 (1999) 56–77.
[4] X. Feng, G.E. Fryxell, L.-Q. Wang, A.Y. Kim, J. Liu, K.M. Kemmer, Science 276 (1997) 923–926.
[5] C.-G. Wu, T. Bein, Chem Mater. 6 (1994) 1109–1112.
[6] E. Armngol, M.L. Cano, A. Coma, H. Garcia, M.T. Navarro, J. Chem. Soc., Chem. Commun. (1995) 519–520.
[7] K.A. Koyano, T. Tatsumi, Y. Tanaka, S. Nakata, J. Phys. Chem. B 101 (1997) 9436–9440.
[8] T. Tatsumi, K.A. Koyano, Y. Tanaka, S. Nakata, J. Porous Mater. 6 (1999) 13–17.
[9] X.S. Zhao, F. Audsley, G.Q. Lu, J. Phys. Chem. B 102 (1998) 4143–4146.
[10] C.-Y. Chen, S.-Q. Xiao, M.E. Davis, Microporous Mater. 4 (1995) 1.
[11] J.M. Kim, J.H. Kwak, S. Jun, R. Ryoo, J. Phys. Chem. 99 (1995) 16742–16747.
[12] D. Cas, C.-M. Tsai, S. Cheng, J. Chem. Soc., Chem. Commun. (1999) 473–474.
[13] N. Coustel, F.D. Renzo, F. Fajula, J. Chem. Soc., Chem. Commun. (1994) 967–968.
[14] R. Mokaya, W. Zhou, W. Jones, J. Chem. Commun. (1999) 51–51.
[15] D.T. On, S.M.J. Zaidi, S. Kaliaguine, Microporous Mesoporous Mater. 22 (1998) 211–224.
[16] R. Mokaya, W. Jones, J. Mater. Chem. 9 (1999) 555–561.
[17] J.C. Vartuli, K.D. Schmitt, C.T. Kresge, W.J. Roth, M.E. Leonowicz, S.B. McCullen, S.D. Hellring, J.S. Beck, J.L. Schlenker, D.H. Olson, E.W. Sheppard, Chem. Mater. 6 (1994) 2317–2326.
[18] Q. Huo, D.I. Margolese, G.D. Stucky, Chem. Mater. 8 (1996) 1147–1160.
[19] S. Brunnauer, P.H. Emmet, E. Teller, J. Am. Chem. Soc. 60 (1938) 309.
[20] S. Brunnauer, L.S. Deming, W.S. Deming, E. Teller, J. Am. Chem. Soc. 62 (1940) 1723.
[21] P.T. Tanev, L.T. Vlaev, J. Colloid Interface Sci. 160 (1993) 110.
[22] H. Naono, M. Hakuman, K. Nakal, J. Colloid Interface Sci. 165 (1994) 532.
[23] E.P. Barrett, L.G. Joyner, P.P. Halenda, J. Am. Chem. Soc. 73 (1951) 373.
[24] S.S. Kim, W. Zhang, T.J. Pinnavaia, Science 282 (1998) 1302–1305.
[25] E. Prouzet, F. Cot, G. Nabias, A. Larbot, K. Patricia, T. Pinnavaia, J. Chem. Mater. 11 (1999) 1498–1503.
[26] P.T. Tanev, T.J. Pinnavaia, Science 267 (1995) 865–867.
[27] Z. Luan, C. Cheng, W. Zhou, J. Klinowski, J. Phys. Chem. 99 (1995) 1018.
[28] A. Monnier, F. Schuth, Q. Huo, D. Kumar, D. Margolese, R.S. Maxell, G.D. Stucky, M. Krishnamurty, P. Petroff, A. Firouzi, M. Janicke, B.F. Chmelka, Science 261 (1993) 1299.